

certainty calculations often produces poor uncertainty estimations.

A copy of the compiled SDS program can be obtained from the author by sending \$15 to cover the costs of handling and mailing (specify 3½- or 5¼-in. disk).

### Acknowledgment

The author is indebted to the referees for valuable comments and suggestions.

## Examining the Shapes of Atomic Orbitals Using Mathcad

**B. Ramachandran**

Louisiana Tech University  
Ruston, LA 71272

One of the more difficult aspects of atomic structure theory at the undergraduate level lies in understanding the specific roles played by the radial and angular parts of hydrogenic wave functions in giving the atomic orbitals their three-dimensional shapes. We recently described a way to generate three-dimensional contour surfaces of atomic orbitals using Mathematica (6). However, Mathematica is a rather expensive package that runs on expensive hardware, and its user interface may seem somewhat intimidating to the first-time user.

This article describes how three-dimensional contour plots of spherical harmonics, that is, surfaces on which  $|Y_{lm}|$  is constant, may be generated using Mathcad, versions 4.0 or higher. Mathcad is relatively inexpensive, runs on inexpensive PC's, and has a very intuitive user interface. Not surprisingly, several applications of Mathcad in teaching Chemistry have appeared in *this Journal* (7-10).

### The Roles of Spherical Harmonics and Radial Functions

The three-dimensional plots of the real spherical harmonics (formed by superpositions of the complex ones where necessary) are very closely related to the three-dimensional shapes of atomic orbitals that do not have radial nodes, that is, the 1s, 2p, 3d, etc. Therefore, this exercise will clarify the role of the spherical harmonics in determining the shapes of the atomic orbitals. The role of the radial functions can then be introduced (perhaps using Mathematica) to complete the picture.

Figure 7 shows a typical exercise in graphing a three-dimensional surface using the absolute value of the angular part of the  $2p_x$  orbital, that is,

$$\left| \frac{Y_{1,1} + Y_{1,-1}}{2} \right| = 1$$

The notes, which can be placed anywhere in the document, can make the exercise self-contained and self-explanatory. The "live document" feature of Mathcad allows one to generate a different atomic orbital simply by redefining the array  $Y_{lm_{i,j}}$ . For example, Figure 8 shows the surface on which  $|Y_{20}| = 1$ , obtained by redefining  $Y_{lm_{i,j}}$  in Figure 7.

One may also use the ideas outlined above and in the two figures to generate the shapes of hybrid atomic orbitals.

We generate the three  $sp^2$  hybrid orbitals and represent them graphically.

$$i = 0..30 \quad \theta_i = \frac{\pi \cdot i}{30} \quad j = 0..40 \quad \phi_j = \frac{2 \cdot \pi \cdot j}{40}$$

The two  $p$  orbitals are represented by the corresponding spherical harmonics. The  $s$  orbital can be represented simply by a constant:

$$px_{i,j} = \sin(\theta_i) \cdot \cos(\phi_j) \quad py_{i,j} = \sin(\theta_i) \cdot \sin(\phi_j)$$

Define the three hybrid orbitals, using the  $S$  orbital radius to be 1/3:

$$\text{The first hybrid orbital, } sp^2(1): \quad sp21_{i,j} := \left| \frac{0.333}{\sqrt{3}} + \frac{2}{\sqrt{3}} px_{i,j} \right|$$

$$\text{The second hybrid orbital, } sp^2(2): \quad sp22_{i,j} := \left| \frac{0.333}{\sqrt{3}} - \frac{1}{\sqrt{6}} px_{i,j} - \frac{1}{\sqrt{2}} py_{i,j} \right|$$

$$\text{The third hybrid orbital, } sp^2(3): \quad sp23_{i,j} := \left| \frac{0.333}{\sqrt{3}} - \frac{1}{\sqrt{6}} px_{i,j} + \frac{1}{\sqrt{2}} py_{i,j} \right|$$

Define the  $x, y, z$  coordinates for the parametric plots:

$$\begin{aligned} x1_{i,j} &= sp21_{i,j} \cdot \sin(\theta_i) \cdot \cos(\phi_j) & x2_{i,j} &= sp22_{i,j} \cdot \sin(\theta_i) \cdot \cos(\phi_j) \\ y1_{i,j} &= sp21_{i,j} \cdot \sin(\theta_i) \cdot \sin(\phi_j) & y2_{i,j} &= sp22_{i,j} \cdot \sin(\theta_i) \cdot \sin(\phi_j) \\ z1_{i,j} &= sp21_{i,j} \cdot \cos(\theta_i) & z2_{i,j} &= sp22_{i,j} \cdot \cos(\theta_i) \end{aligned}$$

$$\begin{aligned} x3_{i,j} &= sp23_{i,j} \cdot \sin(\theta_i) \cdot \cos(\phi_j) \\ y3_{i,j} &= sp23_{i,j} \cdot \sin(\theta_i) \cdot \sin(\phi_j) \\ z3_{i,j} &= sp23_{i,j} \cdot \cos(\theta_i) \end{aligned}$$

Now plot  $(x1, y1, z1)$  for the first hybrid orbital,  $(x2, y2, z2)$  for the second, and  $(x3, y3, z3)$  for the third. By keeping the "tilt" and "rotations" the same for all three, their relative orientations are clearly observable.

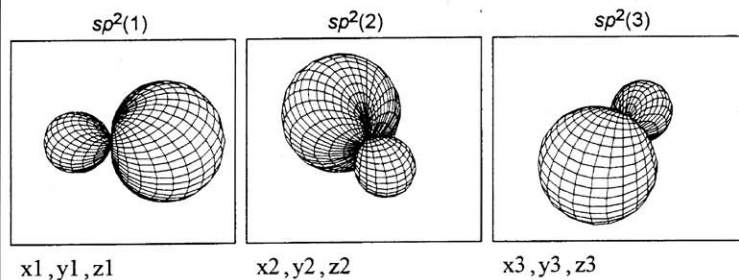


Figure 9. Use of Mathcad to generate the shapes of the three  $sp^2$  hybrid atomic orbitals.

This is a particularly useful exercise because the role of the superpositions of atomic orbitals in giving the hybrid orbitals their shapes and orientation is rather nonintuitive. Figure 9 illustrates one such exercise, where the three  $sp^2$  hybrid orbitals are generated using the linear combinations of the  $2s$ ,  $2p_x$ , and  $2p_y$  orbitals. All three are plotted at  $0^\circ$  rotation and  $45^\circ$  tilt (see the graph menu of Mathcad) so that their relative orientations are due to  $sp^2(1)$ ,  $sp^2(2)$ ,

and  $sp^2(3)$ , whereas their shapes are due entirely to the superpositions used to form the constructive and destructive interference of the spherical harmonics.

In the superpositions, the 2s orbital is represented by the constant 0.333. Because all contour surfaces are for  $|Y_{lm}| = 1$ , the maximum radius of the spheroidal surface is 1 in all cases. However, the shapes of the hybrid orbitals formed by linear combinations of atomic orbitals depend crucially on the relative spatial extents of the orbitals, which are controlled by the radial parts of the wave functions. In forming the  $sp^2$  hybrids shown in Figure 9, we have limited the radius of the 2s orbital to 1/3, whereas the 2p orbitals have a maximum radius of 1. This ratio of the relative radii was chosen because the ratio of

$$4\pi r^2 |\Psi_{2s}|^2 \text{ to } 4\pi r^2 |\Psi_{2p}|^2$$

is exactly 1:3 at the radius where  $4\pi r^2 |\Psi_{2p}|^2$  reaches its maximum value. This choice is, however, rather arbitrary, and one could choose any other value. For pedagogic reasons, however, it is perhaps better to limit the range of possible values so that the resulting hybrid orbitals bear some resemblance to the sketches shown in the textbooks.

There is no provision in Mathcad to display the Cartesian axes in parametric surface plots. There also appears to be no easy way to superimpose two or more parametric plots so that all three hybrid orbitals may be shown in a single plot.

#### Acknowledgment

This work was derived from the project "Enhancement of Physical Chemistry Courses", funded by the Louisiana Education Quality Support Fund, contract no. LEQSF (I 993-94)-ENH-TR-22.

### Computation of Vapor Pressure

#### Ravinder Abrol

Indian Institute of Technology  
Kanpur - 208 016 India

Maxwell (11) has suggested a means for determining the vapor pressures from the isotherms of the analytical cubic equations of state. A typical isotherm is shown in Figure 10. The vapor pressure is indicated by the dashed line  $AE$ . When 1 mol of the liquid is transformed into its vapor, the change in the Gibbs free energy ( $\Delta G$ ) is given by

$$\Delta G = G_{\text{vapor}} - G_{\text{liquid}} = \int V dp \quad (1)$$

Here the integration is along  $ABCDE$ , the S-shaped curve. Under the equilibrium conditions,  $G_{\text{vapor}}$  equals

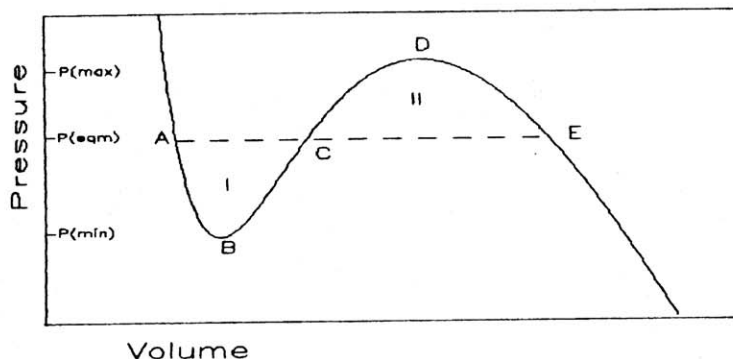


Figure 10. A typical isotherm.

$G_{\text{liquid}}$ , so the integral in eq 1 is zero. This requires the tie-line  $AE$  to be chosen so that area I of the region bounded by the line  $AC$  and the curve  $ABC$  is equal to area II bounded by the line  $CE$  and the curve  $CDE$ .

#### A Simple FORTRAN Program for PC's

We have used the above idea to develop a simple computational program in FORTRAN 77 that computes the vapor pressures for any cubic equation of state using the exact Cardan's solution of a cubic polynomial. Students can learn a lot about analytical equations of state and phase equilibrium by doing such computations; they can compare the accuracy of different cubic equations of state for various temperature ranges. The program is very easy to use and can be run on relatively inexpensive hardware (PC with a 486SX processor). It requires only the temperature of interest and the gas constants as inputs. Noggle and Wood (12) proposed an approach using Mathematica; it used compiled programs and was just a blackbox to the student.

#### Algorithm

First, we take an equation of state, for example, the van der Waals (VDW) equation,

$$P = \frac{RT}{(V-b)} - \frac{a}{V^2} \quad (2)$$

We differentiate  $P$  in eq 2 with respect to  $V$  and equate it to zero to find the  $P_{\text{max}}$  and  $P_{\text{min}}$  values  $D$  and  $B$  in Figure 10. So we get the following cubic equation in  $V$ .

$$RTV^3 - 2aV^2 + 4abV - 2ab^2 = 0 \quad (3)$$

Equation 3 is solved for  $V$  using Cardan's solution of a cubic polynomial, which gives exact roots. The three computed values of  $V$  are used in eq 2 to give three values of pressure; only the higher two correspond to points  $D$  and  $B$  in Figure 10 (i.e.,  $P_{\text{max}}$  and  $P_{\text{min}}$ ), and the lowest must be ignored always.

Equation 2 is rewritten as

$$pV^3 - (pb + RT)V^2 + aV - ab = 0 \quad (4)$$

Equation 4 is solved for pressures in the range  $P_{\text{max}}$  to  $P_{\text{min}}$ , using Cardan's solution. The three values of  $V$  thus obtained (i.e.,  $V_1, V_2, V_3$ ) are used to compute area I and area II (refer to Fig. 10), given by

$$\text{area I} = p(V_2 - V_1) - RT \log \left( \frac{V_2 - b}{V_1 - b} \right) - a \left( \frac{1}{V_2} - \frac{1}{V_1} \right) \quad (5)$$

$$\text{area II} = RT \log \left( \frac{V_3 - b}{V_2 - b} \right) + a \left( \frac{1}{V_3} - \frac{1}{V_2} \right) - p(V_3 - V_2) \quad (6)$$

$$\text{ratio} = \frac{\text{area II}}{\text{area I}} \quad (7)$$

The pressure for which the ratio becomes very close to unity is reported as the equilibrium vapor pressure at the temperature of the isotherm.

#### Results and Discussion

For various gases like  $\text{CO}_2$ ,  $\text{H}_2$ ,  $\text{O}_2$ ,  $\text{H}_2\text{O}$ , etc., treated as VDW gases, the percentage error has been around 0–4% for the temperatures close to the critical temperatures ( $T_c$ ). For example, for  $\text{H}_2$  at 32 K the computed value is 1120.8 kPa, and the experimental value is 1119.7 kPa. This shows that the VDW equation is a good equation of state at temperatures close to the  $T_c$ , and the boiling point can also be predicted with very good accuracy.